Communication

Spinodal Decomposition Mechanism of γ' Precipitation in a Single Crystal Ni-Based Superalloy

X.P. TAN, D. MANGELINCK, C. PERRIN-PELLEGRINO, L. ROUGIER, CH.-A. GANDIN, A. JACOT, D. PONSEN, and V. JAQUET

The precipitation of γ' phase in a commercial single crystal Ni-based superalloy with different cooling rates has been investigated by atom probe tomography. Numerous irregular interconnected γ' precipitates in the size range of ~30 to 50 nm were obtained even utilizing the fastest possible cooling rate. Diffuse γ/γ' interface and far from equilibrium composition of γ' phase were observed in the fast-cooled sample, suggesting that γ' precipitation occurs *via* a spinodal decomposition at the very early stage.

DOI: 10.1007/s11661-014-2506-8

AM1 is a commercial single crystal Ni-based superalloy, which has been extensively used as the materials for high-pressure gas turbine blades and vanes in various aircraft engines.[1] It belongs to the first generation Re-free single crystal Ni-based superalloys. Its microstructure consists of cuboidal γ' precipitates embedded into the γ matrix after standard heat treatment.[1,2] It is subjected to a three-step heat treatment, *i.e.*, solution, primary aging, and secondary aging heat treatments. The alloy is first solutionized at the single γ field, and then cooled to precipitate a $L1_2$-ordered γ' phase from the face-centered cubic (fcc) γ matrix. The cooling rate after solutionizing mainly determines the size, the morphology, and the distribution of γ' precipitates. It is followed by the primary and secondary aging heat treatments at an intermediate temperature and a low temperature, which allows to refine the size and the morphology of γ' precipitates.[3]

The precipitation of γ' phase has been widely studied in various Ni-based alloys, *e.g.*, Ni-Al alloys,[4–9] Ni-Al-Cr alloys,[10–12] Ni-Al-Ti alloys,[13–15] polycrystalline superalloys,[16–21] *etc.* However, very few papers have been involved in the study of γ' precipitation in single crystal Ni-based superalloys at early stage during the rapid cooling conditions. Since γ' phase has a $L1_2$ ordered structure, γ' phase separation must be accompanied by an ordering process. However, it still remains debatable with respect to the occurrence sequence of the spinodal clustering and atomic ordering. The chemical ordering would precede the spinodal decomposition due to the short-range atomic jump involved in the ordering process while long-range diffusion is needed for spinodal decomposition.[22,23] Many literatures dealing with low supersaturated Ni-Al,[4,5,8] Ni-Al-Cr systems,[10,11] or simplified superalloy[16] reported that the initial γ' precipitation occurs by classical nucleation. Nevertheless, Hill and Ralph[9] carried out a combined high-resolution transmission electron microscopy (HRTEM) and atom probe field-ion microscopy (APFIM) study of a Ni-14.1 at. pct Al alloy aged at 898 K (625 °C) and found that the formation of γ' phase involves a continuous phase separation or spinodal decomposition process in conjunction with atomic ordering in terms of the analysis of concentration profiles. Gentry and Fine[6] and Corey *et al.*[7] suggested that the spinodal decomposition or non-classical nucleation was involved in the precipitation of the ordered precipitates. Recent study by Viswanathan *et al.*[20] reported the concomitant spinodal decomposition and chemical ordering in the commercial Ni-based superalloy René 88DT by coupling aberration-corrected scanning transmission electron microscopy (STEM) with atom probe tomography (APT). Therefore, there exists controversy on the mechanisms involved in the γ' precipitation from γ phase. This might be linked to the fact that the decomposition of γ phase in most commercial Ni-based superalloys could not be prohibited due to the large driving force for the precipitation of γ' phase.[17,24] Hence, the study on the initial γ' precipitation in commercial single crystal Ni-based superalloys was found to be much more difficult in comparison to Ni-Al alloys or simplified superalloys. In this paper we thus investigate in detail the γ' precipitation mechanism at the very early stage in single crystal Ni-based AM1 superalloy by means of APT.

As-cast ingots of single crystal Ni-based AM1 superalloy with a composition of Ni-12.15Al-2.41Ta-1.41W-7.15Co-8.55Cr-1.48Ti-1.22Mo (at. pct) were provided by SNECMA (Gennevilliers, France). Solution heat treatment at 1573 K (1300 °C) for 24 hours was performed on single crystal ingots with subsequent air cooling to eliminate the chemical segregation. In order to obtain the fastest possible cooling rate, thin sections of the solution heat-treated samples (~1 mm) were solutionized in the single γ phase field at 1573 K (1300 °C) for half an hour followed by a rapid water quench. The cooling rate was estimated as high as 1273 K/s (1000 °C/s). Moreover, some thin section of

X.P. TAN, formerly with the IM2NP, UMR 7334 CNRS, Université Aix-Marseille, 13397 Marseille Cedex 20, France, is now Research Fellow with the School of Mechanical and Aerospace Engineering, Nanyang Technological University, Singapore 639798, Singapore. Contact e-mail: xptan1985@gmail.com D. MANGELINCK, CNRS Researcher, and C. PERRIN-PELLEGRINO, Lecturer, are with the IM2NP, UMR 7334 CNRS, Université Aix-Marseille. L. ROUGIER, Doctoral Assistant, and A. JACOT, Scientist, are with the LSMX, MXG, Ecole Polytechnique Fédérale de Lausanne, 1015 Lausanne, Switzerland. CH.-A. GANDIN, CNRS Researcher, is with the CEMEF, UMR 7635 CNRS, Mines Paristech, 06904 Sophia Antipolis, France. D. PONSEN and V. JAQUET, Research Engineers, are with the Snecma-SAFRAN Group, Service YQGC, Colombes, France.

Manuscript submitted February 22, 2014.
Article published online August 14, 2014

samples was solutionized at 1573 K (1300 °C) for half an hour followed by a furnace cooling until 973 K (700 °C) and then water quenched. The furnace cooling rate was 274.25 K/s (1.25 °C/s). For comparison, thick sections of solution heat-treated samples (~8 mm) were solutionized at 1573 K (1300 °C) for half an hour and then water quenched. These three samples were termed HC (with the high cooling rate), IC (intermediate cooling rate), and LC (low cooling rate), respectively. In addition, Thermo-Calc™ software with the Ni20 database was used to calculate the equilibrium compositions of γ and γ' phases.[25]

APT samples were prepared by cutting $0.2 \times 0.2 \times 20$ mm^3 rods from HC, IC, and LC samples and electropolishing in a 10 pct perchloric acid in an acetic acid electrolyte at 25 to 30 V and then fine-polishing in a 2 pct perchloric acid in butoxyethanol solution at 5 to 10 V to form needle-shaped tips having a radius of curvature of ~50 nm. APT samples were analyzed by laser-pulsed local-electrode atom probe (LEAP™) at 40 K (−233 °C) and a gauge pressure $<2 \times 10^{-11}$ Torr. Pulses of green laser light (532 nm wavelength) were applied at a 100 kHz repetition rate with an energy of 0.6 nJ pulse^{-1}, yielding an effective evaporation rate of 1.20 pct. Data analysis was performed using IVAS™ 3.6.2 software and compositional information was obtained employing the proximity histogram (proxigram) methodology.[26]

Figure 1 shows the reconstructed volumes obtained by APT for HC, IC, and LC samples. The values of 11 at. pct and 14 at. pct Cr were chosen because they approximately lie midpoint between the Cr concentration in γ and γ' phases in the proxigrams. Figure 1(a) reveals the large amounts of γ' precipitates in the size ranges of ~30 to 50 nm in HC sample. Their number density is 3.32×10^{22} m^{-3}. The size ranges of γ' precipitates become ~70 to 100 nm and >200 nm in IC and LC samples, respectively. Moreover, γ/γ' interfaces appear to be parallel in IC and LC samples, which implies that γ' precipitates tend to be cuboidal with the decreasing cooling rate. In HC sample, γ' precipitates are interconnected and exhibit irregular shape. The widths of γ/γ' interface are 5.8 ± 0.2, 3.2 ± 0.2, and 2.6 ± 0.2 nm for HC, IC, and LC samples respectively, which were defined from the Cr concentration profile in the proxigrams in Figure 2. The error bar associated with the interface width is ±0.2 nm based on the bin size used for computing the proxigrams. In addition, the concentration profiles have to be convoluted by a Gaussian function with a full width at half maximum of ~1 nm,[27] which partly takes into account trajectory aberrations and local magnification effects.[28,29] The concentration profiles are flat in γ' and wavy in γ in HC sample. Of particular interest is its diffuse interface between γ and γ' phase. Therefore, the width of γ/γ' interface evolves from diffuse to sharp with the decrease of cooling rate. In addition, Cr concentration amplitude was found to increase with the increasing time of precipitation. It indicates that the "up-hill" diffusion occurred during the γ' precipitation. Since γ' size is large and γ' volume fraction is high, the variation of concentration amplitude in γ matrix is much larger in comparison to that in γ' phase.

Figure 3 shows the proxigrams for the main elements in HC and LC samples: Al, Ni, Ta, and Ti preferentially

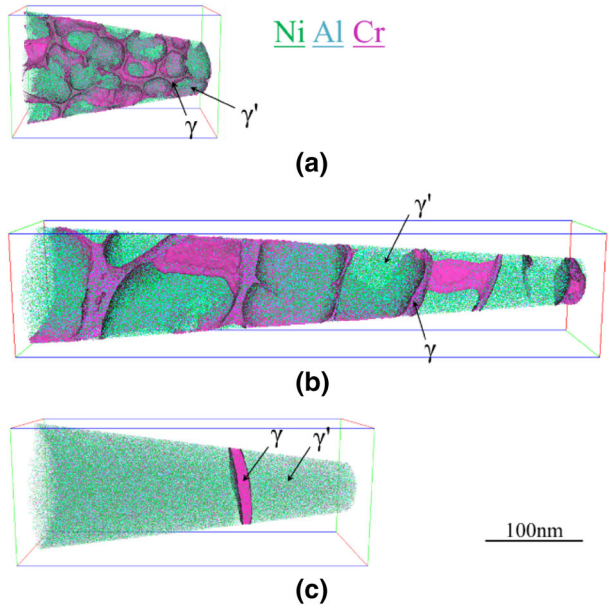

Fig. 1—APT reconstructions showing the γ' precipitates in three AM1 samples after homogenization heat treatment with different cooling rates: (*a*) HC, (*b*) IC, and (*c*) LC. 11 at. pct Cr iso-concentration surfaces (iso-surfaces) were adapted to delineate the γ/γ' interfaces in (a) and 14 at. pct iso-surfaces in (b) and (c).

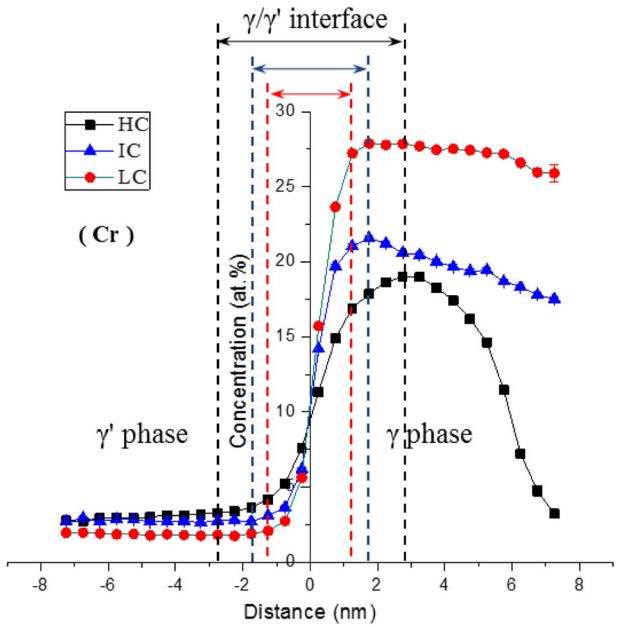

Fig. 2—Proxigram of Cr across the γ/γ' interface delineating with 11 at. pct Cr iso-surfaces in the APT reconstruction of HC sample and 14 at. pct Cr iso-surfaces in IC and LC samples.

partition to γ' phase, while Cr, Co, Mo, and W enter more inside the γ matrix. The concentration profiles of all elements in γ' phase remain flat regardless of γ' size. However, they became flat instead of the initial gradient in the slowly cooled LC sample. Table I reveals that the compositions of γ and γ' phases are far from their equilibrium values in HC sample. Furthermore, both of the compositions of γ and γ' phases tend to be closer to the equilibrium values for LC sample.

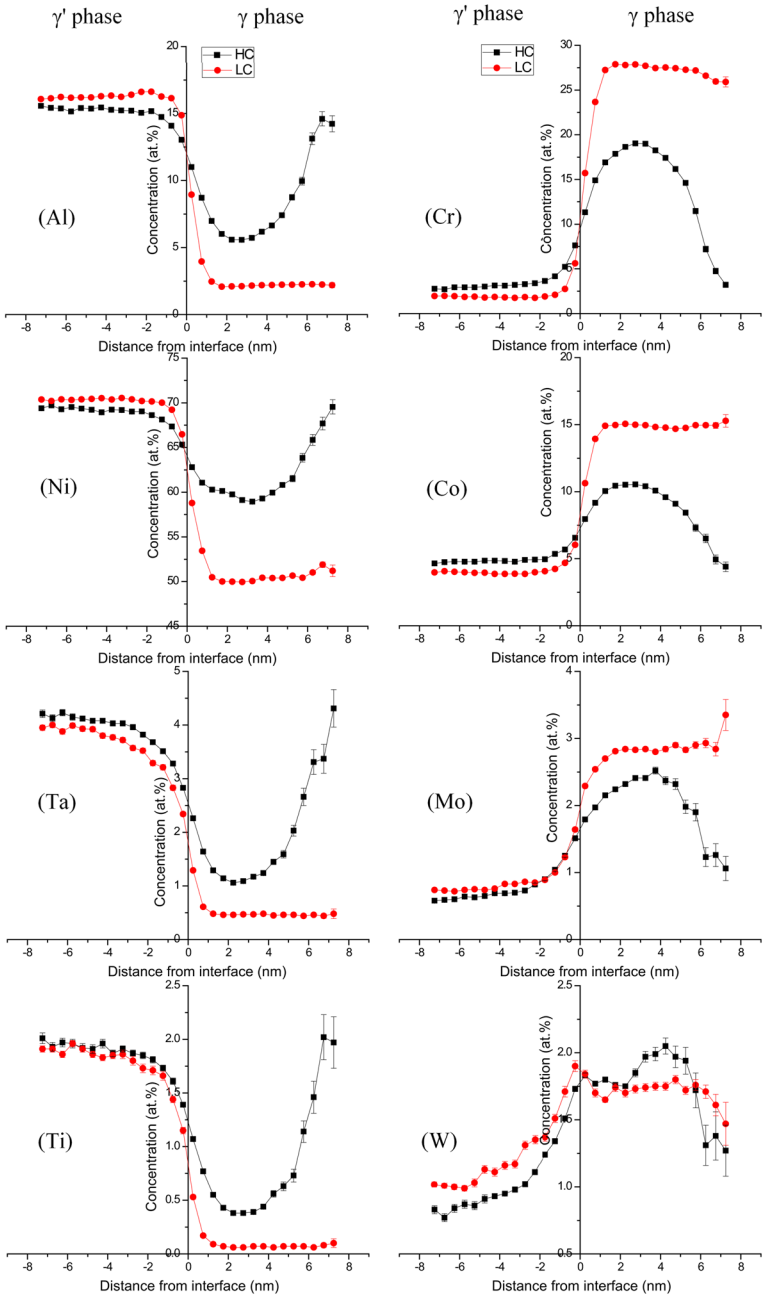

Fig. 3—Proxigrams showing the concentration profiles of the alloying elements across the γ/γ' interface delineating with 11 at. pct Cr iso-surface in the APT reconstruction of HC sample (square) and 14 at. pct Cr iso-surface in LC sample (circle).

A solid solution cooled inside a two-phase domain can decompose by two usual ways: nucleation or spinodal decomposition.[30] Spinodal decomposition occurs for large undercooling or large supersaturation. The solution is unstable because small fluctuation in composition will cause the total free energy to decrease, which takes place in the miscibility region where the free energy curve has a negative curvature.[30–32] A two-phase mixture gradually emerges by the continuous growth of initially small amplitude fluctuation in the inhomogeneous solution. Negative diffusivity, *e.g.*, "uphill" diffusion, and diffuse interface between precipitate and matrix are the main characteristics during the early stage of spinodal decomposition. Moreover, there is no thermodynamic barrier for this transformation process.[30]

It has been well-established both experimentally and theoretically that clustering and ordering are not mutually exclusive processes in undercooled or supersaturated metallic solid solution, but often proceed concomitantly during the decomposition of a quenched alloy.[22,33,34] In particular, Soffa *et al.*[35] analyzed the possible interaction of ordering and clustering tendencies in the formation of an ordered precipitates ($A_3B/L1_2$) within a binary-supersaturated fcc solid solution. Based on the generalized Bragg-Williams model incor-

Table I. The Compositions of γ and γ' Phases in HC and LC Samples Measured by APT and the Equilibrium Compositions at 293 K (20 °C) Calculated by Thermo-Calc Software (at. pct)[25]

	Ni	Al	Ta	W	Co	Cr	Ti	Mo
HC								
γ	59.13 ± 0.10	5.57 ± 0.05	1.09 ± 0.02	1.85 ± 0.03	10.54 ± 0.06	19.03 ± 0.08	0.38 ± 0.01	2.41 ± 0.03
γ'	69.34 ± 0.24	15.38 ± 0.12	4.14 ± 0.06	0.86 ± 0.05	4.78 ± 0.07	2.92 ± 0.14	1.95 ± 0.03	0.62 ± 0.04
LC								
γ	50.86 ± 0.55	2.23 ± 0.02	0.46 ± 0.01	1.69 ± 0.11	14.91 ± 0.20	26.84 ± 0.69	0.07 ± 0.02	2.94 ± 0.19
γ'	70.37 ± 0.10	16.18 ± 0.07	3.92 ± 0.07	1.04 ± 0.05	3.97 ± 0.07	1.89 ± 0.07	1.89 ± 0.04	0.74 ± 0.01
Equilibrium								
γ	38.58	8.88E−8	1.00E−10	6.37	25.8	25.4	2.44E−9	3.80
γ'	75.00	15.91	3.58	0.22	2.24E−3	2.89	2.03	0.37

Table II. Initial Supersaturation of the Experimental AM1 Alloy Assuming an Infinite Quenching Rate from the Homogenization Temperature[25]

	Al	Ta	W	Co	Cr	Ti	Mo
Ω_i	0.76	0.67	0.81	0.72	0.75	0.73	0.75

porating first and second nearest-neighbor interaction, the free energy $F(C, \eta)$ of mixing of a solution with pure components A and B can be formulated as the function of composition C and order parameter η[35]:

$$F(C,\eta) = NC(1-C)(12V+6U) + \frac{3N}{16}\eta^2(4V-6U) - TS_{\mathrm{M}},$$

where N is the total number of atoms of A and B, V and U are the interchange energies associated with first and second nearest-neighbor interactions, $-TS_{\mathrm{M}}$ denotes the entropic term, respectively. For negative V and positive U, the $F(C, \eta)$ *vs* C curves can exhibit negative curvature for the ordered phase at a broad composition range, while the curvature always remains positive for the disordered phase. It implies that a disordered supersaturated γ solid solution would spontaneously order and then undergo spinodal decomposition resulting in disordered γ matrix with ordered γ' precipitates when it is quenched under large undercooling and/or supersaturation.

The supersaturation Ω_i can be defined as

$$\Omega_i = \left(C_{0(i)} - C^*_{\gamma(i)}\right) / \left(C^*_{\gamma'(i)} - C^*_{\gamma(i)}\right),$$

where $C_{0(i)}$ is the overall concentration of element (i) in the alloy, $C^*_{\gamma(i)}$ and $C^*_{\gamma'(i)}$ are the equilibrium compositions of γ and γ' phase, respectively. If $\Omega_i \rightarrow 1$, it means that the supersaturation is very high. In this work, the alloy AM1 was solutionized at the single γ phase field and then rapidly quenched to the room temperature. As shown in Table II, the supersaturation of the initial alloy is relatively high. Due to the high supersaturation of the initial alloy, large amounts of irregular γ' precipitates with high connectivity in the size ranges of ~30 to 50 nm were obtained even employing the fastest possible cooling rate. By contrast, no γ' precipitation was obtained for the as-quenched Ni-5.2Al-14.2Cr (at. pct) alloy in the work by Sudbrack *et al.*[10] Our results show that the precipitation of γ' precipitates cannot be prohibited in the commercial single crystal Ni-based superalloy. In addition, the γ/γ' interface is found to be diffuse with a width of γ/γ' interface comparable to the thickness of γ matrix channel. Furthermore, the compositions of γ and γ' phases are far from their equilibrium compositions. The modulation amplitude of concentration profiles becomes markedly larger when increasing the cooling time and thus the precipitation time. All these results suggest that the γ' precipitation occurs *via* concomitant ordering and spinodal decomposition when the alloy is quenched by a very fast cooling rate in AM1 alloy. Similarly, an excellent APT work by Babu *et al.*[17] also indicates that γ' precipitation undergoes a concomitant ordering and spinodal decomposition in water-quenched samples of a commercial CM247DS superalloy, as a high number density of irregular interconnected γ' precipitates was observed. Thanks to state-of-the-art LEAP, however, huge APT reconstructed volumes were obtained in this work, which will be greatly helpful for studying the γ' phase evolution with different cooling rates. Moreover, of particular importance is that our work reveals the very diffuse γ/γ' interface and obvious up-hill diffusion with the aid of proxigram methodology. It is believed to provide strong evidence for spinodal decomposition under a rapid cooling.

The precipitation of γ' phase can thus be explained in terms of the hypothetical phase diagram and free energy schematics in Figure 4, which correspond to alloys that are solution heat-treated at temperature T_1 and then quenched to a temperature T_2. Most of Ni-Al or Ni-Al-X alloys (*e.g.*, Ni-Al-Cr alloys in the work of Sudbrack *et al.*[10,11]) that have been reported in publications correspond to the alloy with composition C_1 that the γ' precipitation occurs *via* the classical nucleation due to the low supersaturation, where the corresponding free energy curves of γ and γ' phase both have positive curvatures. For the commercial Ni-based superalloys, *e.g.*, highly supersaturated AM1 alloy in this work (alloy

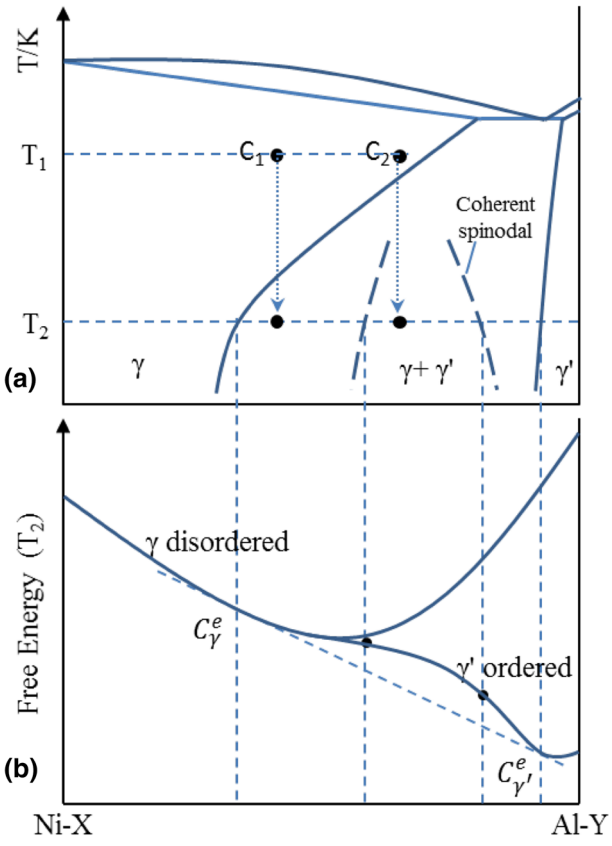

Fig. 4—Schematic illustration of a phase diagram (Ni-rich end) and its corresponding hypothetical free energy-composition diagram for the superalloy that might undergo a transformation *via* concomitant ordering and spinodal decomposition.

with composition C_2 in Figure 4), γ' phase would precipitate *via* concomitant ordering and spinodal decomposition when the alloy was quenched from temperature T_1 to T_2 with a high undercooling. This is due to the fact that its composition is within the hypothetical coherent spinodal region. It is worth pointing out that the accurate phase diagram and free energy curve of commercial superalloys are difficult to obtain because of their complex multicomponent systems. In particular, it is hard to calculate the free energy curve at a very high cooling using current thermodynamic data which are calibrated on equilibrium conditions. As indicated in this work, however, the free energy curve is significant to predict the precipitation mechanism of γ' phase. Thus, further experimental and theoretical work on phase diagrams and free energy curves is quite needed in the multicomponent superalloys.

In summary, the APT characterization of the precipitation of the γ' phase in an AM1 superalloy shows that large amounts of irregular interconnected γ' precipitates in the size range of ~30 to 50 nm were obtained even utilizing the fastest possible cooling rate. A decrease in the cooling rate leads to the following changes: (i) the size of γ' precipitates is increased; (ii) the number density decreases; (iii) the morphology tends to become cuboidal instead of irregular shape. The diffuse γ/γ' interface, the up-hill diffusion of most of the elements, and the interconnected structure strongly indicate that the precipitation of γ' phase occurs *via* concomitant ordering and spinodal decomposition under extremely fast cooling or large undercooling in the commercial single crystal Ni-based AM1 superalloy.

The authors are very grateful to Marion Descoins for APT technical support. Georges Martin is acknowledged for fruitful discussions.

REFERENCES

1. P. Caron and O. Lavigne: *Aerosp. Lab.*, 2011, vol. 3, pp. 1–14.
2. P. Caron and T. Khan: *Aerosp. Sci. Technol.*, 1999, vol. 3, pp. 513–23.
3. X.P. Tan, J.L. Liu, T. Jin, Z.Q. Hu, H.U. Hong, B.G. Choi, I.S. Kim, C.Y. Jo, and D. Mangelinck: *Mater. Sci. Technol.*, 2014, vol. 30, pp. 289–300.
4. A.J. Ardell and R.B. Nicholson: *Acta Metall.*, 1966, vol. 14, pp. 1295–309.
5. A.J. Ardell: *Acta Metall.*, 1968, vol. 16, pp. 511–16.
6. W.O. Gentry and M.E. Fine: *Acta Metall.*, 1972, vol. 20, pp. 181–90.
7. C.L. Corey, B.Z. Rosenblum, and G.M. Greene: *Acta Metall.*, 1973, vol. 21, pp. 837–44.
8. H. Wendt and P. Haasen: *Acta Metall.*, 1983, vol. 31, pp. 1649–59.
9. S.A. Hill and B. Ralph: *Acta Metall.*, 1982, vol. 30, pp. 2219–25.
10. C.K. Sudbrack, K.E. Yoon, R.D. Noebe, and D.N. Seidman: *Acta Mater.*, 2006, vol. 54, pp. 3199–210.
11. C.K. Sudbrack, R.D. Noebe, and D.N. Seidman: *Acta Mater.*, 2007, vol. 55, pp. 119–30.
12. D. Blavette, E. Cadel, C. Pareige, B. Deconihout, and P. Caron: *Microsc. Microanal.*, 2007, vol. 13, pp. 464–83.
13. M. Doi, D. Miki, T. Moritani, and T. Kozakai: in *Superalloys 2004*, K.A. Green, T.M. Pollock, H. Harada, T.E. Howson, R.C. Reed, J.J. Schirra, and S. Walston, eds., TMS, Warrendale, PA, 2004, pp. 109–14.
14. S. Hata, K. Kimura, H. Gao, S. Matsumura, M. Doi, T. Moritani, J.S. Barnard, J.R. Tong, J.H. Sharp, and P.A. Midgley: *Adv. Mater.*, 2008, vol. 20, pp. 1905–09.
15. F. Vogel, N. Wanderka, S. Matsumura, and J. Banhart: *Intermetallics*, 2012, vol. 22, pp. 226–30.
16. S. Chambreland, A. Walder, and D. Blavette: *Acta Metall.*, 1988, vol. 36, pp. 3205–15.
17. S.S. Babu, M.K. Miller, J.M. Vitek, and S.A. David: *Acta Mater.*, 2001, vol. 49, pp. 4149–60.
18. J. Tiley, G.B. Viswanathan, R. Srinivasan, R. Banerjee, D.M. Dimiduk, and H.L. Fraser: *Acta Mater.*, 2009, vol. 57, pp. 2538–49.
19. A.R.P. Singh, S. Nag, J.Y. Hwang, G.B. Viswanathan, J. Tiley, R. Srinivasan, H.L. Fraser, and R. Banerjee: *Mater. Charact.*, 2011, vol. 62, pp. 878–86.
20. G.B. Viswanathan, R. Banerjee, A.R.P. Singh, S. Nag, J. Tiley, and H.L. Fraser: *Scripta Mater.*, 2011, vol. 65, pp. 485–88.
21. A.R.P. Singh, S. Nag, S. Chattopadhyay, Y. Ren, J. Tiley, G.B. Viswanathan, H.L. Fraser, and R. Banerjee: *Acta Mater.*, 2013, vol. 61, pp. 280–93.
22. W.A. Soffa and D.E. Laughlin: *Acta Metall.*, 1989, vol. 37, pp. 3019–28.
23. J.-C. Zhao and M.R. Notis: *Acta Mater.*, 1998, vol. 46, pp. 4203–218.
24. D. Blavette, E. Cadel, and B. Deconihout: *Mater. Charact.*, 2000, vol. 44, pp. 133–57.
25. Ni20: *Ni Base Alloys Database 2010*, Thermo-Calc Software AB.
26. O.C. Hellman, J.A. Vandenbroucke, J. Rüsing, D. Isheim, and D.N. Seidman: *Microsc. Microanal.*, 2000, vol. 6, pp. 437–44.
27. H. Benallali, K. Hoummada, M. Descoins, P. Rueda-Fonseca, L. Gerad, E. Bellet-Amalric, S. Tatarenko, K. Kheng, and D. Mangelinck: *Scripta Mater.*, 2013, vol. 69, pp. 505–08.
28. D. Blavette, A. Bostel, and J.M. Sarrau: *Metall. Trans. A*, 1985, vol. 16A, pp. 1703–11.

29. E. Cadel, D. Lemarchand, S. Chambreland, and D. Blavette: *Acta Mater*., 2002, vol. 50, pp. 957–66.
30. D.A. Porter and K.E. Easterling: *Phase Transformations in Metals and Alloys*, CRC, Boca Raton, FL, 1992.
31. S. Para: *ASM Int*., 2004, vol. 9, pp. 140–43.
32. G. Lesoult: *Thermodynamique des matériaux: De l'élaboration des matériaux à la genèse des microstructures*, Traité des Matériaux Tome, Presses Polytechniques Universitaires Romandes, Lausanne, vol. 5, 2010.
33. H. Ino: *Acta Metall*., 1978, vol. 26, pp. 827–34.
34. A.G. Khachayuryan, T.F. Lindsey, and J.W. Morris: *Metall. Trans. A*, 1988, vol. 19A, pp. 249–58.
35. W.A. Soffa, D.E. Laughlin, and N. Singh: *Phil. Mag*., 2010, vol. 90, pp. 287–304.